UCRL-JRNL-215825

Laurentide Ice Sheet meltwater and abrupt climate change during the last glaciation

H. W. Hill, B. P. Flower, T. M. Quinn, D. J. Hollander, T. P. Guilderson

October 3, 2005

Paleoceanography

Disclaimer

Laurentide Ice Sheet meltwater and abrupt climate change during the last glaciation

Heather W. Hill[1], Benjamin P. Flower[1*], Terrence M. Quinn[1], David J. Hollander[1], Thomas P. Guilderson[2]

[1]College of Marine Science, University of South Florida, St. Petersburg, FL 33701, USA
[2]LLNL Center for Accelerator Mass Spectrometry, University of California, Livermore, CA 94550, USA
Department of Ocean Sciences, and Institute of Marine Sciences, UC Santa Cruz, Santa Cruz CA 95064, USA

*To whom correspondence should be addressed. E-mail: bflower@marine.usf.edu.

Abstract

A leading hypothesis to explain abrupt climate change during the last glacial cycle calls on fluctuations in the margin of the North American Laurentide Ice Sheet (LIS), which may have routed freshwater between the Gulf of Mexico (GOM) and North Atlantic, affecting North Atlantic Deep Water (NADW) variability and regional climate. Paired measurements of $\delta^{18}O$ and Mg/Ca of foraminiferal calcite from GOM sediments reveal five episodes of LIS meltwater input from 28-45 thousand years ago (ka) that do not match the millennial-scale Dansgaard-Oeschger (D/O) warmings recorded in Greenland ice. We suggest that summer melting of the LIS may occur during Antarctic warming and likely contributed to sea-level variability during Marine Isotope Stage 3 (MIS 3).

1. Introduction

Abrupt climate changes during the last glaciation have been linked to variations in Atlantic thermohaline circulation. Numerical models demonstrate that an increased flux of freshwater to sites of deep-water formation decreases the strength of North Atlantic Deep Water (NADW), thereby reducing meridional heat transport and causing cooling/warming in the northern/southern high latitudes [*Ganopolski and Rahmstorf*, 2001; *Knutti et al*., 2004]. This bipolar seesaw [*Broecker*, 1998] has been invoked to explain the anti-phased relationship between climate changes in Antarctica and Greenland, where warmings in Antarctica precede those in Greenland by several thousand years [*Blunier and Brook*, 2001]. Additionally, the climate signature in Antarctica shows gradual temperature changes, while Greenland temperature is characterized by higher frequency changes, including abrupt warmings that occur in decades, followed by slow coolings (Dansgaard-Oeschger (D/O) cycles).

The North American Laurentide Ice Sheet (LIS) may have served as a source of freshwater to the North Atlantic during the last deglaciation, when ice-sheet retreat led to the diversion of freshwater (meltwater and precipitation) from the Mississippi River drainage to the Hudson and St. Lawrence Rivers [*Broecker et al*., 1988; 1989; *Shackleton*, 1989; *Rooth*, 1990; *Flower and Kennett*, 1990; *Clark et al*., 2001; *Flower et al*., 2004]. Meltwater routing has been suggested as a potential control of high-frequency climate variability during intervals of intermediate ice volume, such as during Marine Isotope Stage 3 (MIS 3) [*Clark et al*., 2001]. However, evidence is needed to assess potential switches in freshwater routing during the millennial-scale D/O cycles, which are characterized by 5-10^{o}C oscillations in Greenland air temperature [*Dansgaard et al*., 1993]. Here we test whether D/O warmings correspond to freshwater routing to the Gulf of Mexico (GOM) by reconstructing the $\delta^{18}O$ composition of seawater ($\delta^{18}O_{sw}$) using paired measurements of $\delta^{18}O_{calcite}$ ($\delta^{18}O_c$) and Mg/Ca of GOM foraminifera. Orca Basin (26°56.77'N, 91°20.74'W; Figure 1) in the northern GOM is ideally located to study freshwater input, including LIS meltwater, from the North American continent because of its proximal location to the mouth of the Mississippi River.

2. $\delta^{18}O$ and Mg/Ca Analyses

Core MD02-2551 was recovered from Orca Basin in July 2002 by the R/V *Marion Dufresne* as part of the IMAGES (International Marine Past Global Changes Study) program. The core was sampled at 2 cm intervals from 21-30 m. All samples were freeze-dried prior to wet sieving, and then washed over a 63-_m mesh using deionized water. ~60-70 planktonic foraminifera *G. ruber* (pink variety) were picked from the 250-355 _m size fraction for isotopic and elemental analyses. The foraminifera were sonicated in methanol for five seconds to remove clays, and then weighed to assess downcore dissolution effects. Mean *G. ruber* weights are similar throughout the interval and are comparable to surface-sediment samples [*LoDico*, 2003]. The shells were gently crushed open between two glass plates and carefully homogenized using a razor blade. A ~50 _g aliquot was removed for stable isotopic analysis, which was performed at the College of Marine Science, University of South Florida using a ThermoFinnigan Delta Plus XL dual-inlet mass spectrometer with an attached Kiel III carbonate preparation device. The isotopic data (Figure 2) are reported on the VPDB scale calibrated with NBS-19. Standard deviation for the $\delta^{18}O_c$ measurements is ± 0.04‰, based on measurements of the standard NBS-19 analyzed with MD02-2551 foraminifer samples (n=105).

The remaining tests, weighing ~700 _g, were split into two aliquots that were cleaned separately for Mg/Ca analysis [*Barker et al*., 2003]. This method involves an initial sonication to remove fine clays, oxidation of organic matter with a buffered peroxide solution, and a dilute acid leach that eliminates any adsorbed contaminants. Samples were dissolved in weak HNO_3 to yield calcium concentrations of ~20 ppm to minimize calcium concentration effects. The Mg/Ca ratios (Figure 2) were analyzed on a Perkin Elmer Optima 4300 dual view inductively coupled plasma-optical emission spectrometer (ICP-OES). A standard instrument-drift correction technique was routinely used. The analytical precision for Mg/Ca determinations used in this study is <0.6% root-mean standard deviation (1σ), based on an ICP-MS calibrated standard solution. The pooled standard deviation of 70% replicate Mg/Ca analyses is ± 2.5% (d.f. = 318), which is equivalent to ~0.3^{o}C.

3. Age Model

The age model developed for our record (Figure 2) is based on 18 AMS ^{14}C dates (Table 1) determined from monospecific samples (4-10 mg) of pink *G. ruber*, which were run at the Center for Accelerator Mass Spectrometry, Lawrence Livermore National Laboratory. The ^{14}C ages were corrected for a reservoir age of 400 years and converted to the GISP2 timescale (an approximation of calendar years) using a high-resolution radiocarbon calibration developed on sediment cores from the Cariaco Basin [*Hughen et al*., 2004]. Inferred minimal changes in upwelling indicate uncertainty in the reservoir correction is much better than 100 years. Age was also constrained by the Laschamp geomagnetic event [*Laj et al.*, 2000], which is recorded as a ~50 cm minimum in inclination at a depth of ~27.5 m [*Kissel et al.*, m.s. in prep]. A peak in ^{10}Be, which coincides with the Laschamp event in sediment cores from the North Atlantic [*Robinson et al.*, 1995], straddles the δ^{18}O peak of Interstadial 10 in the Greenland ice core record [*Yiou et al.*, 1997]. The Laschamp event was therefore assigned a calendar age of 40.9 k.a. based on the age of the δ^{18}O peak of Interstadial 10 on the Greenland GISP2 time scale [*Meese et al.*, 1997] (Figure 2).

Depth in centimeters was converted to age by applying a weighted curve fit with a 40% smoothing factor and linearly extrapolating beyond the Laschamp event. This function fits a curve to the calibrated ^{14}C age control points, using the locally weighted Least Squares error method. Because of the uncertainty associated with radiocarbon dates of increasing age, including ^{14}C age plateaus at ~24 and ~28 ^{14}C k.a. [*Hughen et al.*, 2004], the weighted smooth fit provides a conservative estimate of depth vs. age. Sedimentation rates range from 25 cm/k.y. to 325 cm/k.y.

Total error (1_) on the age model ranges from 140 calendar years at ~26 ka to a maximum of 700 calendar years at ~40 ka. Error was determined by compounding the error on the ^{14}C measurements from this study (Table 1), the error on the ^{14}C measurements from the Cariaco record and the error from the GISP2/Cariaco calibration reported by Hughen et al. (2004). Errors in ^{14}C were converted to calendar years using the Cariaco calibration. Calculating the error prior to 40 ka is difficult because of the uncertainty in the Cariaco calibration. Errors on the layer counting from the GISP2 record were not included in the total error analysis because we do not make conclusions about the absolute age of our events. Rather, we place our records on the GISP2 timescale to compare our results to Greenland air temperature history.

We have also placed our data on the newly proposed age scale for the Greenland ice cores (SFCP 2004), which is based on ^{14}C dating of foraminifera in core MD95-2042, calibrated by paired ^{14}C and ^{230}Th measurements on corals [*Shackleton et al*., 2004] (see Supplementary Information). The conclusions that we report in the paper are the same regardless of which timescale we use for the Greenland ice core record.

4. Gulf Of Mexico $\delta^{18}O$ of Seawater

The *G. ruber* $\delta^{18}O_c$ values range from ~ –0.5 to –2.5‰ (Figure 3). This 2‰ variability is not seen in the $\delta^{18}O_c$ of *N. dutertrei* (data not shown), an inferred deep-dwelling planktonic foraminifer, suggesting that surface water phenomena are controlling the $\delta^{18}O_c$. The $\delta^{18}O_c$ record exhibits four oscillations about a mean value of –1.25‰, from 28-45 k.a. (Figure 3). $\delta^{18}O_c$ values are more negative than the modern core-top value of pink *G. ruber* (–1.7‰) during two of these oscillations (28.7-29.2 k.a. and 37.3-39.8 k.a., Figure 3). Given that sea level was 63-93 m below present from 30-45 k.a. [*Siddall et al*., 2003], which would result in an enrichment of the foraminifera $\delta^{18}O_c$ by ~0.5-0.75‰ based on the relationship 0.083‰ per 10m sea-level change [*Adkins et al*., 2001], $\delta^{18}O_c$ values ≤–1.7‰ would indicate SSTs of 30-32°C during MIS 3, which are unreasonably high compared to the modern average summer temperature in the GOM (29°C; June-Sep) [*Levitus*, 2003]. A change in $\delta^{18}O_{sw}$ associated with salinity variations is therefore required to explain the four negative oscillations recorded in the foraminiferal calcite.

In order to isolate $\delta^{18}O_{sw}$, we subtract the temperature component from the $\delta^{18}O_c$ based on Mg/Ca data [*Flower et al*., 2004]. The Mg/Ca ratio, a proxy for the temperature of foraminiferal calcification, is ideal for $\delta^{18}O_{sw}$ calculations because it is measured on an aliquot of the calcite sample used for $\delta^{18}O_c$. A *G. ruber* (pink) calibration, based on Atlantic sediment trap data [*Anand et al*., 2003], was applied to the Mg/Ca measurements to calculate SST (Figure 3). We make the assumption that the effect of riverine input on the Mg/Ca values is minimal based on the large difference in Mg and Ca concentrations in the Mississippi River and the GOM (425 _M Mg vs. 53 mM Mg; 870 _M Ca vs. 10.3 mM Ca; *Briggs and Ficke*, 1978). Despite the lower Mg/Ca ratio of Mississippi River water, oceanic Mg/Ca is not likely to be affected because the concentrations of Mg/Ca are low. A simple box model calculation shows that a 25% dilution of surface seawater (a likely maximum for *G. ruber* to withstand; *Hemleben et al*., 1989) would only decrease Mg/Ca values by <3%, which is within measurement error.

The Mg-SST component was removed from the $\delta^{18}O_c$ using a temperature- $\delta^{18}O$ relationship [*Bemis et al*., 1998] appropriate for *G. ruber* [*Thunell et al*., 1999], resulting in the $\delta^{18}O_{sw}$. The standard deviation for $\delta^{18}O_{sw}$ calculations is determined to be ± 0.25‰, based on propagating the error through the analytical errors and the combined Mg-SST and SST-$\delta^{18}O$ relationships [*Beers*, 1957]. The variances used for the Mg-SST and SST-$\delta^{18}O$ equations are those reported in the literature. Variances for Mg/Ca and $\delta^{18}O$ were based on replicate analyses.

The $\delta^{18}O_{sw}$ variations from core MD02-2551 have similarities to the global sea-level record from MIS 3 [*Siddall et al*., 2003] (Figure 3). However sea-level fluctuations of <30 m during this interval [*Siddall et al*., 2003] can explain only 0.25‰ of the >1‰

$\delta^{18}O_{sw}$ changes observed in our record, suggesting that changes in evaporation/precipitation (E-P) or freshwater input must be the dominant control on the $\delta^{18}O_{sw}$. We use the sea-level record [*Siddall et al*., 2003] to remove the contribution of global ice volume to the $\delta^{18}O_{sw}$, leaving the GOM $\delta^{18}O_{sw}$ residual ($\delta^{18}O_{GOM}$) (Figure 4). This was accomplished by converting sea-level height to the $\delta^{18}O$ equivalent using the relationship 0.0083‰ per 1m sea-level change [*Adkins et al*., 2001].

$\delta^{18}O_{GOM}$ values reflect changes in salinity, which result from a combination of source-water variability and/or changes in the volume of water affecting the $\delta^{18}O_{GOM}$ signal. The $\delta^{18}O_{GOM}$ oscillates by up to 1.5‰, between more fresh versus more saline conditions, about a mean value of 0.45‰ (Figure 4). Major freshwater events, defined as intervals when the $\delta^{18}O_{GOM}$ reach values <0.45‰ and persist for >1 k.a., occurred from 31.6-33.9 k.a. and 37.3-39.8 k.a (F2 and F4; Figure 4). The signatures of these two freshwater events are different, however: F2 is defined by a gradual change from more saline to more fresh conditions, while F4 is characterized by an abrupt freshening and an abrupt return to saline conditions. Three minor freshwater events, from 28.4-29.3, 35.0-35.6 and 42.9-43.7, also record values < 0.45‰, but persist for <1 k.a. (F1, F3 and F5; Figure 4).

5. Conversion to Sea-surface Salinity

Conversion of $\delta^{18}O_{GOM}$ estimates to sea-surface salinity (SSS) allows us to assess potential sources and magnitudes of freshwater flux to the GOM. SSS can be estimated using a $\delta^{18}O_{GOM}$ versus salinity relationship created for the GOM during MIS 3 (Figure 5). This relationship assumes conservative mixing between two end-members: high salinity GOM waters ($\delta^{18}O_{sw}$ = 1.2‰ and S = 36.5 psu) and a low salinity end-member. The low salinity end-member is modeled using three different compositions: 1) 1) a –3.5‰ value for GOM precipitation [*Bowen and Revenaugh*, 2003], and a Laurentide Ice Sheet (LIS) value ranging from 2) –15‰, reflecting the $\delta^{18}O$ of source waters that drained from the LIS [*Yapp and Epstein*, 1977], to 3) –30‰, the average composition of the LIS [*Dansgaard et al.*, 1969]. It should be noted that the more negative the zero salinity intercept, the smaller the changes in the estimated salinity variations (Figure 5). For example, a 1‰ change in $\delta^{18}O_{GOM}$ is equivalent to ~1 psu on the -30‰ LIS mixing line, ~2 psu on the -15‰ LIS mixing line and ~8 psu on the –3.5‰ MR mixing line.

Use of the -3.5‰ end-member would require changes in salinity of up to 10 psu (Figure 6) and a volume of water 3-5 times the largest historical flood [*Barry*, 1997], or >50X the annual precipitation in the GOM [*Ropelewski et al.*, 1996], lasting for 3 k.y. during the largest event. It is possible that the isotopic composition of continental precipitation draining into the Mississippi River was more negative during MIS 3, due to changes in the altitude and/or sources of precipitation. However, a minimal change in the $\delta^{18}O$ composition of precipitation during MIS 3 is inferred from model simulations, which show similar $\delta^{18}O$ precipitation values between the Last Glacial Maximum and present [*Charles et al.*, 2001]. In addition, mid-continent speleothems, which reflect the changing isotopic composition of meteoric waters, record <0.5‰ variations in $\delta^{18}O$ during this interval [*Dorale et al.*, 1998]. We cannot rule out the possibility that increased precipitation over the GOM may reflect an intensification of the North American monsoon system, which is known to bring moisture to the region. However, the amount necessary to create the observed changes in the $\delta^{18}O_{GOM}$ record does not support oceanic precipitation as a primary control on this signal. In contrast, meltwater derived from the LIS with a $\delta^{18}O$ composition of –15 to –30‰ would require only modest changes in salinity: a –15‰ end-member for the LIS results in a salinity change of up to 3.5 psu, while a –30‰ end member results in a change in salinity of up to 2 psu (Figure 6). Additionally, the average SSS using a -30‰ endmember is 35.5 ± 1 psu, which is within the modern salinity range in the GOM.

We recognize that the source of fresh water likely changed through time and may have been a mixture of various sources (ie. meltwater and precip), and therefore the SSS calculations only reflect the endmember scenarios. Regardless, the most conservative estimate for salinity changes indicates a substantial meltwater contribution to $\delta^{18}O_{sw}$ in the GOM, particularly when the $\delta^{18}O$ composition of GOM waters were most depleted . This explanation is supported by recent reconstructions of the LIS during MIS 3, which place the margin of the ice sheet within the MR drainage basin [*Dyke et al.*, 2002].

6. LIS Routing Hypothesis

The uncertainty in the calibration of ^{14}C to calendar years precludes firm phase comparisons, but there appears to be no consistent relationship between $\delta^{18}O_{GOM}$ freshwater input and Greenland interstadials. The LIS routing hypothesis would predict that the nine D/O warmings (IS 4-12) that span 28-45 k.a. [*Grootes et al.*, 1993] should correspond to freshwater routing to the GOM [*Clark et al.*, 2001], but only five $\delta^{18}O_{GOM}$ freshwater events are recorded in the Orca Basin during this interval (Figure 4). There is no age model that we can construct with the ^{14}C dates that would allow the $\delta^{18}O_{GOM}$ record from Orca Basin to be on the same timing as the D/O cycles in Greenland. In addition, the Laschamp event coincides with a warming in Greenland (IS 10), but a positive $\delta^{18}O$ excursion (more saline) in our record. If each of the D/O warmings corresponds to freshwater routing to the GOM, we would expect to see a negative $\delta^{18}O_{GOM}$ excursion in our record during this interval. Although freshwater routed to eastern outlets may have led to NADW reductions and coolings in Greenland, the timing and number of $\delta^{18}O_{GOM}$ freshwater events to the GOM suggest that a simple routing hypothesis cannot explain all of the MIS 3 Greenland interstadials. It appears that the D/O warmings cannot be attributed to changes in the strength of NADW associated with southward routing of meltwater by the LIS, which may help explain why it has been difficult to find NADW changes during each of the D/O cycles (*Curry et al*., 1999; *Hagen and Keigwin*, 2002; *Vautravers et al*., 2004). Additionally, SST in the GOM does not appear to be coupled to Greenland air temperature.

The $\delta^{18}O_{GOM}$ record has similarities to the Antarctic air temperature record [*Johnsen et al*., 1972], the global sea-level record from MIS 3 [*Siddall et al*., 2003], and to the classic MIS 3 benthic $\delta^{18}O$ record off Portugal [*Shackleton et al*., 2000]. Freshwater events in the GOM have a tendency to coincide with intervals of Antarctic warming. In particular, the largest freshwater event (F4) occurred at the same time as the largest warming in Antarctica (A1 centered at 39 ka; Figure 4) and a 30-m rise in sea level also at 39 ka [*Siddall et al*., 2003].

Our $\delta^{18}O_{GOM}$ record suggests summer melting on the southern margin of the LIS during Antarctic warming, as also observed during the last deglaciation (*Flower et al*., 2004). This provides evidence to support a recent modeling study that suggests that the northern hemisphere ice sheets contributed one-half of the global sea-level rises observed between 35-65 k.a. [*Rohling et al*., 2004]. Our results are also consistent with a new coupled atmosphere-ocean simulation that predicts that freshwater discharge into the Gulf of Mexico would contribute to Antarctic warming [*Knutti et al*., 2004]. LIS melting associated with the A1 warming in Antarctica may have provided a positive feedback for Southern Hemisphere warming through changes in the strength of NADW. Similarly, our results indicate that growth/decay cycles of the LIS may have been decoupled from Greenland air temperature history during MIS 3. Our finding underscores recent work suggesting that the LIS (which is influenced by summer melting) does not follow Greenland air temperature (which is influenced by winter temperatures, particularly during stadials) and that seasonality is an important aspect of abrupt climate change (*Denton et al*., 2005).

Acknowledgements

We thank the IMAGES program for collection of the core. Ethan Goddard provided technical assistance with data collection. We also thank Luis Garcia-Rubio for assistance with error analysis, Richard Poore and Kelly Kilbourne for comments on the manuscript, and Jyotika Virmani, Gary Mitchum, and the USF Paleo lab members for useful discussions. Radiocarbon analyses were performed under the auspices of the U.S. Department of Energy by the University of California Lawrence Livermore National Laboratory (contract W-7405-Eng-48).

Data Archive

Supporting data will be available electronically at World Data Center-A for Paleoclimatology, NOAA/NGDC, 325 Broadway, Boulder, CO 80303, USA, or by phone at 303-457-6513, e-mail: paleo@mail.ngdc.noaa.gov; URL: http://www.ngdc.noaa.gov/paleo.

References

Adkins, J.R., and D.P. Schrag (2001), Pore fluid constraints on deep ocean temperature and salinity during the last glacial maximum, *Geophys. Res. Lett.*, *28*, 771-774.

Anand, P., H. Elderfield, H., and M.H. Conte (2003), Calibration of Mg/Ca thermometry in planktonic foraminifera from a sediment trap time series, *Paleoceanography*, *18*, doi: 10.1029/2002PA000846.

Barker, S., M. Greaves, and H. Elderfield (2003), A study of cleaning procedures used for foraminiferal Mg/Ca paleothermometry, *Geochem., Geophys., Geosyst.*, *4*, doi: 10.1029/2003GC000559.

Barry, J.M. (1997), *Rising Tide-The Great Mississippi Flood of 1927 and How it Changed America*, 524 pp., Simon and Schuster, New York.

Beers, Y. (1957), *Introduction to the Theory of Error*, 66 pp., Addison-Wesley-Longman, Rading, Mass.

Bemis, B.E., J.H. Spero, J. Bijma, and D.W. Lea (1998), Reevaluation of the oxygen isotopic composition of planktonic foraminifera: Experimental results and revised paleotemperature equations, *Paleoceanography*, *13*, 150-160.

Blunier, T., and E.J. Brook (2001), Timing of millennial-scale climate change in Antarctic and Greenland during the last glacial period, *Science*, *291*, 109-112.

Bowen, G.J., and J. Revenaugh (2003), Interpolating the isotopic composition of modern meteoric precipitation, *Water Resources Res.*, *39*, doi: 10.1029/2003WR002086.

Briggs, J.C., and J.F. Ficke (1978), Quality of rivers of the United States, 1975 water year, *Open File Rep. 78-200*, 436 pp., U.S. Geological Survey.

Broecker, W.S., M. Andree, W. Wolfli, H. Oeschger, G. Bonani, J. Kennett, and D. Peteet (1988), The chronology of the last deglaciations: Implications to the cause of the Younger Dryas event, *Paleoceanography*, *3*, 1-19.

Broecker, W.S., J.P. Kennett, B.P. Flower, J.T. Teller, S. Trumbore, G. Bonani, and W. Wolfli (1989), Routing of meltwater from the Laurentide ice sheet during the Younger Dryas cold episode, *Nature*, *341*, 318-321.

Broecker, W.S. (1998), Paleocean circulation during the last deglaciation: A bipolar seesaw?, *Paleoceanography*, *13*(2), 119-121.

Charles, C.S., D. Rind, R. Healy, and R. Webb (2001), Tropical cooling and the isotopic composition of precipitation in general circulation model simulations of the ice age climate, *Climate Dynamics*, *17*(7), 489-502.

Clark, P.U., S.J. Marshall, G.K.C., Clarke, S.W. Hostetler, J.M. Licciardi, and J.T. Teller (2001), Freshwater forcing of abrupt climate change during the last glaciation, *Science*, *293*, 283-287.

Curry, W.B., T.M. Marchitto, J.F. McManus, D.W. Oppo, and K.L. Laarkamp (1999), Millennial-scale changes in ventilation of the thermocline, intermediate, and deep water of the glacial North Atlantic, in *Mechanisms of Global Climate Change at Millennial Time Scales*, edited by P.U. Clark, R.S. Webb, and L.D. Keigwin, pp. 59-76, AGU Washington, D.C.

Dansgaard, W., and H. Tauber (1969), Glacier Oxygen-18 Content and Pleistocene Ocean Temperatures, *Science*, *166*, 499-502.

Dansgaard, W., et al. (1993), Evidence for general instability of past climate from a 250-kyr ice-core record, *Nature*, *364*, 218-220.

Denton, G.H., R.B. Alley, G.C. Comer, and W.S. Broecker (2005), The role of seasonality in abrupt climate change, *Quat. Sci. Rev.*, *24*, 1159-1182.

Dorale, J.A., R.L. Edwards, E. Ito, and L.A. Gonzalez (1998), Climate and vegetation history of the mid-continent from 75 to 25 ka: A speleothem record from Crevice Cave, Missouri, USA, *Science*, *282*, 1871-1874.

Dyke, A.S., J.T. Andrews, P.U. Clark, J.H. England, G.H. Miller, J. Shaw, and J.J. Veillette (2002), The Laurentide and Innuitian ice sheets during the Last Glacial Maximum, *Quat. Sci. Rev.*, *21*, 9-31.

Flower, B.P., and J.P. Kennett (1990), The Younger Dryas cool episode in the Gulf of Mexico, *Paleoceanography*, *5*(6), 949-961.

Flower, B.P., D.W. Hastings, H.W., Hill, H.W., and T.M. Quinn (2004), Phasing of degalcial warming and Laurentide Ice Sheet meltwater in the Gulf of Mexico, *Geology*, *32*, 597-600.

Ganopolski, A., and S. Rahmstorf (2001), Rapid changes of glacial climate simulated in a coupled climate model, *Nature*, *409*, 153-158.

Grootes, P.M., M. Stuiver, J.W.C. White, S. Johnsen, and J. Jouzel (1993), Comparison of oxygen-isotope records from the GISP2 and GRIP Greenland ice cores, *Nature*, *366*, 552-554.

Hagen, S., and L.D. Keigwin (2002), Sea-surface temperature variability and deep water reorganization in the subtropical North Atlantic during Isotope Stage 2-4, Marine *Geology*, *189*, 145-162.

Hemleben, Ch., M. Spindler, and O.R. Anderson (1989), *Modern Planktonic Foraminifera*, 363 pp., Springer-Verlag, New York.

Hughen, K., S. Lehman, J. Southon, J. Overpeck, O. Marchal, C. Herring, and J. Turnbull (2004), ^{14}C Activity and Global Carbon Cycle Changes over the Past 50,000 Years, *Science*, *303*, 202-207.

Johnsen, S.J., H.B. Clausen, W. Dansgaard, and C.C. Langway (1972), Oxygen isotope profiles through Antarctic and Greenland ice sheets, *Nature*, *235*, 429-434.

Knutti, R., J. Fluckiger, T.F. Stocker, and A. Timmermann (2004), Strong hemispheric coupling of glacial climate through freshwater discharge and ocean circulation, *Nature*, *430*, 851-856.

Laj, C., C. Kissel, A. Mazaud, J.E.T. Channell, and J. Beer (2000), North Atlantic Paleointensity Stack since 75 ka (NAPIS-75) and the duration of the Laschamp event, *Philos. Transact. Ser. A Math Phys. Eng. Sci.*, *358*, 1009-1025.

Levitus, S. (2003), National Oceanographic Data Center World Ocean Atlas 1994 at http://www.cdc.noaa.gov/ (NCDC, Boulder, Colorado, USA)

LoDico, J.M., D.W. Hastings, B.P. Flower, and T.M. Quinn (2002), A multi-proxy approach to distinguish between changes in SST and meltwater input in the Gulf of Mexico back to MIS 3, *Eos Trans. AGU*, *83*(47), Fall Meet. Suppl., Abstract PP62A-0331.

Meese, D.A., A.J. Gow, R.B. Alley, G.A. Zielinski, P.M. Grootes, M. Ram, K.C. Taylor, P.A. Mayewski, and J.F. Bolzan (1997), The Greenland Ice Sheet Project 2 depth-age scale: Methods and results, *J. Geophys. Res.*, *102*, 26411-26423.

Robinson, C., G.M. Raisbeck, F. Yiou, B. Lehman, and C. Laj (1995), The relationship between ^{10}Be and geomagnetic field strength records in central North Atlantic sediments during the last 80 ka, *Earth Planet. Sci. Lett.*, *136*, 551-557.

Rohling, E.J., R. Marsh, N.C. Wells, M. Siddall, and N.R. Edwards (2004), Similar meltwater contributions to glacial sea level changes from Antarctic and northern ice sheets, *Nature*, *430*, 1016-1021.

Rooth, C.G.H. (1990), Hydrology and ocean circulation, *Prog. Oceanogr.*, *11*, 131-149.

Ropelewski, C.F., and M.S. Halpert (1996), Quantifying Southern Oscillation-Precipitation relationships, *J. Climate*, *9*, 1043-1059.

Shackleton, N.J. (1989), Deep trouble for climate change, *Nature*, *342*, 616-617.

Shackleton, N.J., M.A. Hall, and E. Vincent (2000), Phase relationships between millennial-scale events 64,000-24,000 years ago, *Paleoceanography*, *15*(6), 565-569.

Shackleton, N.J., R.G. Fairbanks, T. Chiu, T., and F. Parrenin (2004), Absolute calibration of the Greenland time scale: implications for Antarctic time scales and for $\Delta^{14}C$, *Quat. Sci. Rev.*, *23*, 1513-1522.

Siddall, M., E.J. Rohling, A. Almogi-Labin, C. Hemleben, D. Meischner, I. Schmelzer, and D.A. Smeed (2003), Sea-level fluctuations during the last glacial cycle, *Nature*, *423*, 853-858.

Thunnell, R., E. Tappa, C. Pride, C., and E. Kincaid (1999), Sea-surface temperature anomalies associated with the 1997-1998 El Nino recorded in the oxygen isotope composition of planktonic foraminifera, *Geology*, *27*, 843-846.

Vautravers, M.J., N.J. Shackleton, C. Lopez-Martinez, and J.O. Grimalt (2004), Gulf Stream variability during marine isotope stage 3, *Paleoceaongraphy*, *19*, doi: 10.1029/2003PA000966.

Yapp, C.J., and S. Epstein (1977), Climatic implications of D/H ratios of meteoric water over North America (9,500-22,000 B.P.) as inferred from ancient wood cellulose C-H hydrology, *Earth Planet. Sci. Lett.*, *34*, 333-350.

Yiou, F.G., et al. (1997), Beryllium 10 in the Greenland Ice Core Project ice core at Summit, Greenland, *J. Geophys. Res.*, *103*, 26783-26794.

Figure Captions

Figure 1. Map of Orca Basin in the Gulf of Mexico showing location of core MD02-2551 (26º56.77'N, 91º20.74'W, 2248 m water depth) and the extent of the Laurentide Ice Sheet during MIS 3 (from *Dyke et al*., 2002).

Figure 2. Raw $\delta^{18}O_c$ and Mg/Ca data and age model for MD02-2551. a, $\delta^{18}O_c$ shown with 5-point smooth and b, Mg/Ca data shown with 5-point smooth on *G. ruber* from Orca Basin core MD02-2551 vs. depth in the core. c, Age model for our interval based on 18 ^{14}C dates from *G. ruber*, which were converted to the GISP2 timescale (an approximation of calendar years) using a Cariaco Basin radiocarbon calibration [*Hughen et al*., 2004]. Age was constrained by the Laschamp geomagnetic event [*Laj et al*., 2000], which is recorded as a sharp peak in inclination at a depth of ~27.5 m, as indicated by light grey bar (*Kissel et al*., m.s. in prep).

Figure 3. Paired $\delta^{18}O_c$ and Mg/Ca data on *G. ruber* from Orca Basin core MD02-2551 (26º56.77'N, 91º20.74'W, 2248 m water depth) during MIS 3. a. *G. ruber* $\delta^{18}O_c$, shown with 5-point smooth. Mean value indicated by horizontal bar. b. *G. ruber* Mg/Ca converted to SST using Mg/Ca=0.38exp[0.09 X SST (ºC)] [*Anand et al*., 2003]. c. Calculated $\delta^{18}O_{sw}$ from $\delta^{18}O_c$ and Mg-SST using $T(^oC) = 14.9-4.8*(\delta^{18}O_c - \delta^{18}O_{sw})$ [*Bemis et al*., 1998]. 0.27‰ was added to convert to VSMOW. d. Global sea-level record [*Siddall et al*., 2003]. Numbers refer to $\delta^{18}O_c$ oscillations referred to in text. Triangles on the bottom refer to intervals with ^{14}C dates.

Figure 4. Comparison of Orca Basin $\delta^{18}O_{GOM}$ during MIS 3 with ice core records. a. GISP2 $\delta^{18}O_{ice}$ [*Grootes et al*., 1993]. b. Orca Basin $\delta^{18}O_{GOM}$, with mean value indicated by horizontal bar. $\delta^{18}O_{GOM}$ was calculated by subtracting global ice volume from the $\delta^{18}O_{sw}$ record. c. Byrd $\delta^{18}O_{ice}$ record [*Johnsen et al*., 1972] on the GISP2 timescale, based on synchronization of methane concentrations within the two ice cores [*Blunier and Brook*, 2001]. Numbers refer to Greenland interstadials. Light grey bars and the letter F (numbered 1-5) indicate freshwater events referred to in the text. Dark grey bars and letter H indicate Heinrich events. A1 refers to Antarctic warming event number 1 [*Blunier and Brook*, 2001].

Figure 5. Mixing model for the GOM during MIS 3. The $\delta^{18}O_{GOM}$ versus salinity relationship assumes conservative mixing between two end-members: high salinity GOM waters ($\delta^{18}O_{sw}$ = 1.2‰ and S = 36.5 psu) and a low salinity end-member. The low salinity end-member is modeled using three different compositions: a. –3.5‰ for GOM precipitation [*Bowen and Revenaugh*, 2003], b. –15‰, reflecting the $\delta^{18}O$ of source waters that drained from the LIS [*Yapp and Epstein*, 1977], and c. –30‰, the average composition of the LIS [*Dansgaard and Tauber*, 1969].

Figure 6. GOM sea-surface salinity (SSS) reconstructions from 28-45 k.a. SSS is based on the conversion of $\delta^{18}O_{GOM}$ to salinity using a mixing model with three freshwater end-members (see Figure 5). a. $\delta^{18}O_{GOM}$. b. estimated salinity. The most conservative estimate for salinity changes indicates a substantial meltwater contribution to $\delta^{18}O_{sw}$ in the GOM.

Table 1. Radiocarbon Ages for MD02-2551.

CAMS[a] #	Core depth (m)	^{14}C AMS age (k.a.)	^{14}C Error (+/-)	Calibrated age (k.a.)
108325	19.68	23.11	160	26.40
108326	20.16	23.46	70	26.70
108327	20.62	24.22	80	27.30
90835	21.25	25.41	130	28.90
108328	22.02	25.48	90	29.00
100591	22.86	25.54	130	29.05
100592	23.20	24.21	120	27.25
100593	23.60	26.28	140	29.70
100594	24.06	26.79	150	30.00
100595	24.42	27.30	160	30.20
90836	24.75	31.17	250	34.95
100596	25.10	29.59	210	33.30
100597	25.48	31.84	270	35.50
100598	25.90	33.67	340	38.10
108329	26.48	34.20	600	39.20
90837	26.84	33.28	320	37.45
100599	27.22	35.66	420	40.55
Laschamp event	27.50			40.90
100600	27.58	36.23	460	40.75
100601	28.06	35.38	410	40.30[b]
100665	28.46	34.80	500	40.00[b]
108330	29.20	37.83	300	41.30[b]
108331	29.88	33.17	180	37.30[b]

[a]Center for Accelerator Mass Spectrometry (CAMS), Lawrence Livermore National Laboratory

[b]Samples not included in the age model due to stratigraphic inconsistencies. The ^{14}C ages at depths of 28.06, 28.46, and 29.88 m are younger than higher depths in the core. We choose not to use the ^{14}C age at 29.20 because it would require very large sedimentation rate changes from 30 cm/k.y. to 200 cm/k.y. Although this is possible, we instead choose to linearly extrapolate beyond the Laschamp event and are conservative with interpretations in our data prior to 41 k.a.


LIS extent at
27-30 ^{14}C ka BP
N
Orca Basin
Gulf of Mexico
0
500 km

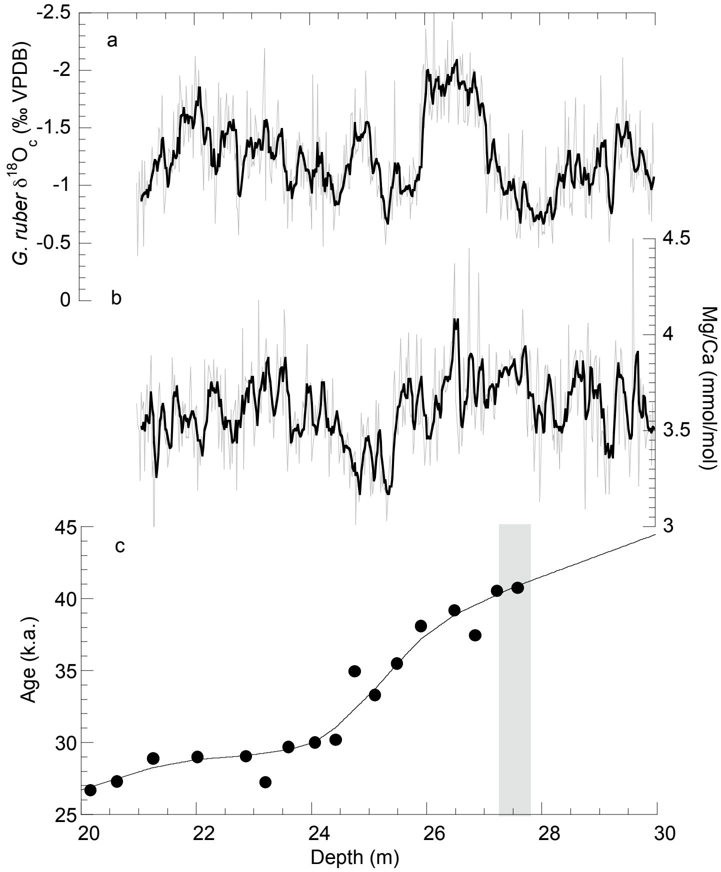

a
b
c
G. ruber δ18Oc (‰ VPDB)
Mg/Ca (mmol/mol)
Age (k.a.)
Depth (m)
-2.5
-2
-1.5
-1
-0.5
0
4.5
4
3.5
3
45
40
35
30
25
20
22
24
26
28
30

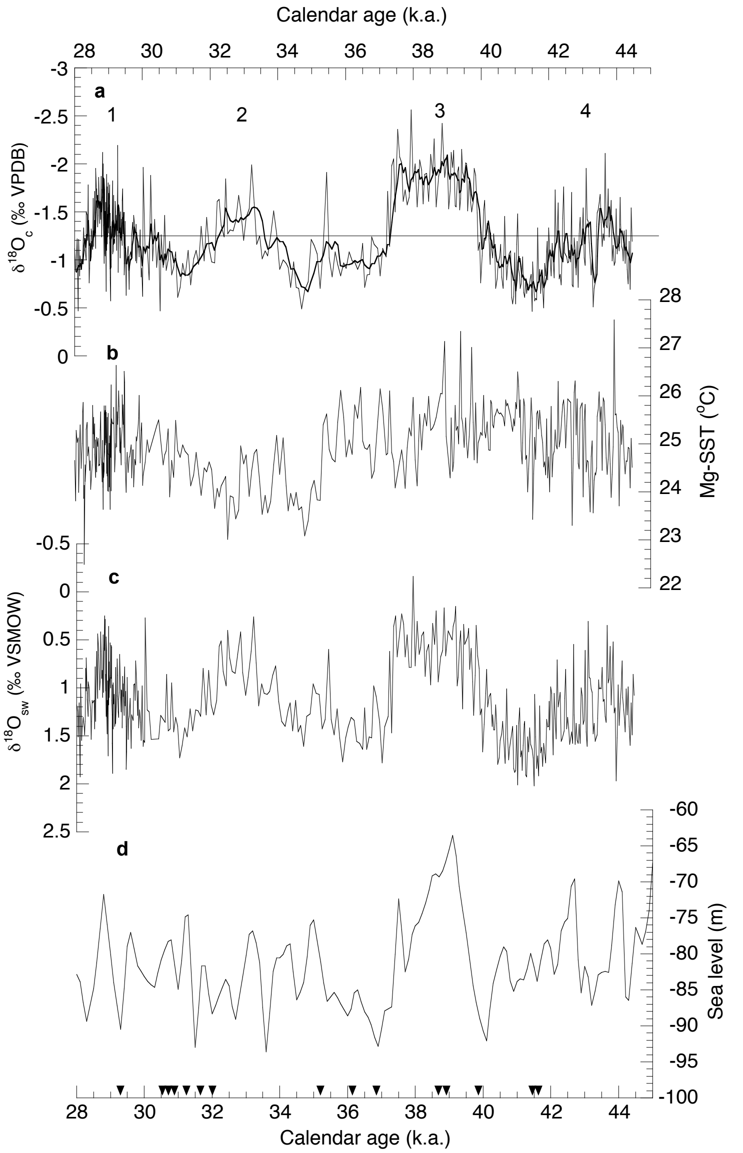
Calendar age (k.a.)
a
b
c
d
1
2
3
4
δ18Oc (‰ VPDB)
Mg-SST (°C)
δ18Osw (‰ VSMOW)
Sea level (m)
Calendar age (k.a.)

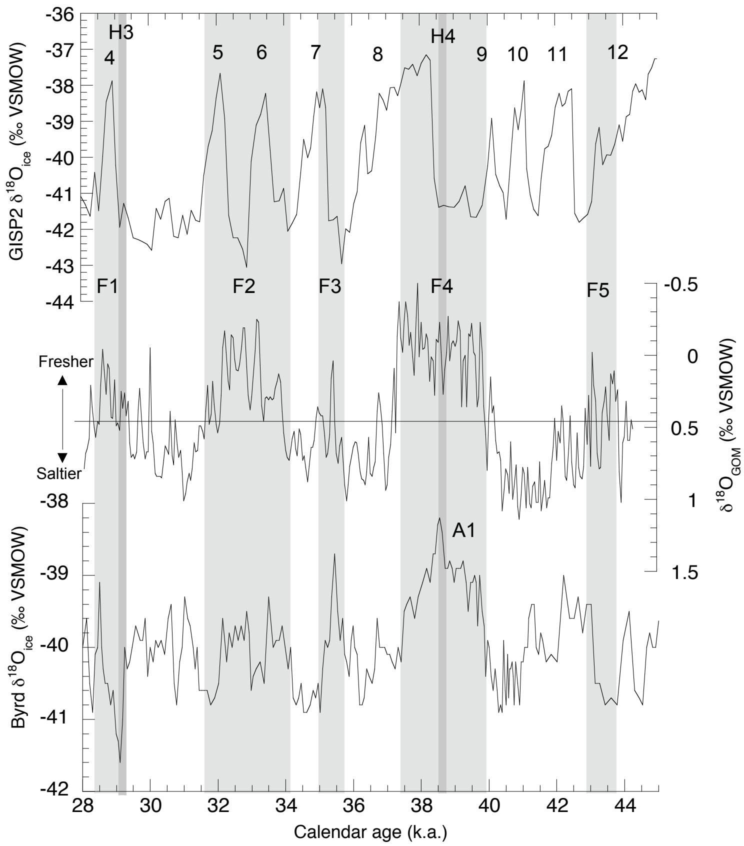

GISP2 $\delta^{18}O_{ice}$ (‰ VSMOW)
-36
-37
-38
-39
-40
-41
-42
-43
-44
H3
4
5
6
7
8
H4
9
10
11
12
F1
F2
F3
F4
F5
-0.5
0
0.5
1
1.5
$\delta^{18}O_{GOM}$ (‰ VSMOW)
Fresher
Saltier
A1
Byrd $\delta^{18}O_{ice}$ (‰ VSMOW)
-38
-39
-40
-41
-42
28
30
32
34
36
38
40
42
44
Calendar age (k.a.)

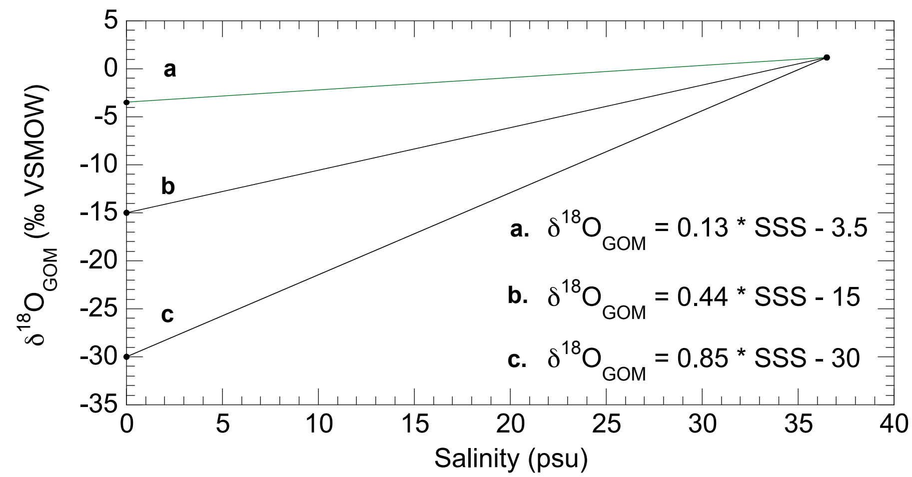

a
b
c
a. $\delta^{18}O_{GOM}$ = 0.13 * SSS - 3.5
b. $\delta^{18}O_{GOM}$ = 0.44 * SSS - 15
c. $\delta^{18}O_{GOM}$ = 0.85 * SSS - 30
$\delta^{18}O_{GOM}$ (‰ VSMOW)
Salinity (psu)

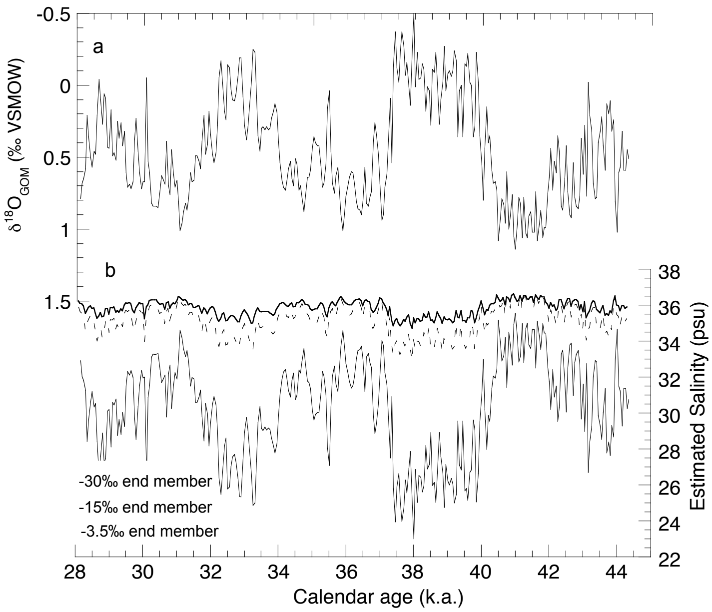

a
b
δ18O GOM (‰ VSMOW)
-0.5
0
0.5
1
1.5
Estimated Salinity (psu)
38
36
34
32
30
28
26
24
22
-30‰ end member
-15‰ end member
-3.5‰ end member
28
30
32
34
36
38
40
42
44
Calendar age (k.a.)

Supplementary Information

We have also placed our data on the newly proposed age scale for the Greenland ice cores (SFCP 2004), which is based on ^{14}C dating of foraminifera in core MD95-2042, calibrated by paired ^{14}C and ^{230}Th measurements on corals [*Shackleton et al*., 2004]. This was done by first applying the SFCP timescale to the Cariaco record (Shackleton, per comm., 2004) and to the global sea-level record [*Siddall et al*., 2003]. The sea-level record was originally correlated to the Byrd $\delta^{18}O$ record using a series of tie points. We used the same tie points to correlate the sea-level record to the Vostok δD record, which has been placed on the SFCP timescale. The relationship of the $\delta^{18}O_{GOM}$ record to the Greenland and Antarctic air temperature records on the SFCP timescale (SI Figure 1) is consistent with the conclusions reported in the paper.

SI Figure 1. Comparison of Orca Basin $\delta^{18}O_{GOM}$ on the SFCP timescale during MIS 3 with ice core records. a, GRIP $\delta^{18}O_{ice}$ [*Johnsen et al*., 2001] on SFCP timescale b, Orca Basin $\delta^{18}O_{GOM}$, with mean value indicated by horizontal bar. $\delta^{18}O_{GOM}$ was calculated by subtracting global ice volume from the $\delta^{18}O_{sw}$ record. c, Vostok δD [*Petit et al*., 1999] on SFCP timescale which is normalized to remove the linear trend. Numbers refer to Greenland interstadials. Light grey bars and the letter F (numbered 1-5) indicate freshwater events referred to in the text. Dark grey bars and letter H indicate Heinrich events. A1 refers to Antarctic warming event number 1 [*Blunier and Brook*, 2001].

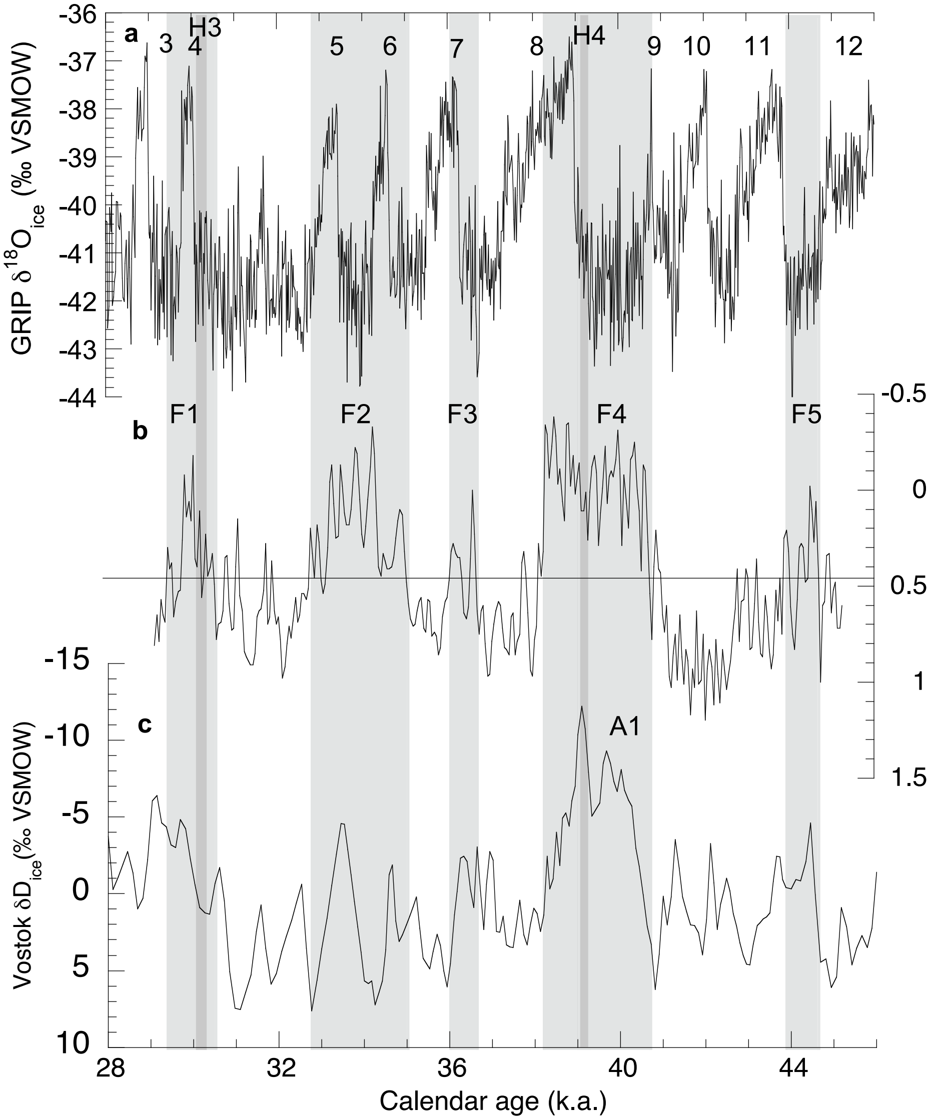

a
b
c
3
4
H3
5
6
7
8
H4
9
10
11
12
F1
F2
F3
F4
F5
A1
GRIP δ18Oice (‰ VSMOW)
δ18OGOM (‰ VSMOW)
Vostok δDice (‰ VSMOW)
Calendar age (k.a.)
-36
-37
-38
-39
-40
-41
-42
-43
-44
-0.5
0
0.5
1
1.5
-15
-10
-5
0
5
10
28
32
36
40
44

References

Blunier, T., and E.J. Brook (2001), Timing of millennial-scale climate change in Antarctic and Greenland during the last glacial period, *Science*, *291*, 109-112.

Johnsen, S.J., et al. (2001), Oxygen isotope and palaeotemperature records from six Greenland ice-core stations: Camp Century, Dye-3, GRIP, GISP2, Renland and NorthGRIP, *Journal of Quaternary Science*, *16*(4), 299-307.

Petit, J.R., et al. (1999), Climate and atmospherica history of the past 420,000 years from the Vostok ice core, Antarctica, *Nature*, *399*, 429-436.

Shackleton, N.J., R.G. Fairbanks, T. Chiu, T., and F. Parrenin (2004), Absolute calibration of the Greenland time scale: implications for Antarctic time scales and for $\Delta^{14}C$, *Quat. Sci. Rev.*, *23*, 1513-1522.

Siddall, M., E.J. Rohling, A. Almogi-Labin, C. Hemleben, D. Meischner, I. Schmelzer, and D.A. Smeed (2003), Sea-level fluctuations during the last glacial cycle, *Nature*, *423*, 853-858.